

RSC Advances



This is an *Accepted Manuscript*, which has been through the Royal Society of Chemistry peer review process and has been accepted for publication.

Accepted Manuscripts are published online shortly after acceptance, before technical editing, formatting and proof reading. Using this free service, authors can make their results available to the community, in citable form, before we publish the edited article. This *Accepted Manuscript* will be replaced by the edited, formatted and paginated article as soon as this is available.

You can find more information about *Accepted Manuscripts* in the [Information for Authors](#).

Please note that technical editing may introduce minor changes to the text and/or graphics, which may alter content. The journal's standard [Terms & Conditions](#) and the [Ethical guidelines](#) still apply. In no event shall the Royal Society of Chemistry be held responsible for any errors or omissions in this *Accepted Manuscript* or any consequences arising from the use of any information it contains.

Functionalized Boron Nitride Porous Solids

P. M. Sudeep^{1,#}, S. Vinod^{2,#}, S. Ozden², R. Sruthi², Akos Kukovecz^{3,4}, Zoltan Konya^{3,5}, Robert Vajtai², M. R. Anantharaman⁶, P. M. Ajayan^{2,*}, and Tharangattu N. Narayanan^{1,*}

¹TIFR- Centre for Interdisciplinary Sciences, Tata Institute of Fundamental Research, Hyderabad-500075, India.

²Materials Science and NanoEngineering Department, Rice University, Houston, TX, USA

³Department of Applied and Environmental Chemistry, University of Szeged, H-6720 Szeged, Rerrich Bela ter 1., Hungary.

⁴MTA-SZTE “Lendület” Porous Nanocomposites Research Group, University of Szeged, H-6720 Szeged, Rerrich Bela ter 1., Hungary.

⁵MTA-SZTE Reaction Kinetics and Surface Chemistry Research Group, University of Szeged, H-6720 Szeged, Rerrich Bela ter 1., Hungary.

⁶Department of Physics, Cochin University of Science and Technology, Kochi-682022, Kerala, India.

*Corresponding author tnn@tifrh.res.in or tn_narayanan@yahoo.com , ajayan@rice.edu

These authors are equally contributed.

Abstract

Hexagonal boron nitride (h-BN), white graphene in the inorganic regime, is well known for its chemical inertness. Recent studies indicate that functionalization of h-BN can tune its physico-chemical properties, including its electrical conductivity. Here we propose a method for the functionalization of h-BN flakes with various oxygen functionalities to make graphite oxide analogue of h-BN, in a view to develop cross-linked, low-density ($\sim 40 \text{ mg/cm}^3$), and porous h-BN solids, as it is recently well cited for graphene and graphite oxide. For the first time, macro-porous low density h-BN monolith foam is developed *via* a single step template free chemical route followed by a lyophilisation process. h-BN is known for its high thermal stability, and here the oil adsorption by the foam ($\sim 2 \text{ g/g}$) and complete burning of the adsorbed oil without disrupting the h-BN skeleton are demonstrated indicating the flexibility of tuning the morphology of h-BN in bulk, like graphite, without losing its inherent physical properties, opening new avenues for h-BN in energy and environment related fields.

Keywords: Macro-porous solids, h-Boron Nitride, Oil adsorption, Thermal stability, Chemical functionalization.

Ever since the discovery of graphene, research on other 2-dimensional (2D) atomic layers has been always on the increase [1]. A number of two dimensional layered materials based on dichalcogenides, perovskites, transition metal oxides and hexagonal boron nitride (h-BN) have garnered immense popularity due to their exciting thermal, mechanical and electronic properties [2-4]. Hexagonal boron nitride (h-BN), a wide bandgap layered insulator, known for its chemical inertness and thermal stability [5], is receiving tremendous attention for its applicability in electronics and thermal management [6]. Though an electrically insulating material [7], h-BN is identified as the best ever known substrate for high carrier mobility graphene, [8] and is widely used for the bandgap engineering of graphene [9]. h-BN is an ideal candidate for optical components, super hydrophobic surface coatings, substrates for electronic devices, mechanical composites and catalysis as well [10-13]. Though pristine h-BN is an insulator, upon fluorination it is found to be becoming conducting, and this enables the functionalized h-BN as a potential platform for electronic devices [14].

Chemical functionalization of h-BN is a challenge due to its high chemical stability. It was reported that water assisted exfoliated h-BN flakes contain small amount of oxygen functional groups [15]. But studies show that the extent of functionalization is negligible so that efficient cross-linking of individual sheets using the external cross-linking agents, as we reported for graphene oxide [16-18], is almost impossible. Other non-covalent functionalization approaches include the functionalization of h-BN nanostructures with amine, phosphine and polymers [19-21]. The resulting linkages are attributed to the π - π interactions and the interactions between boron and nitrogen. Coleman *et.al* proposed a double step method for the covalent functionalization of exfoliated h-BN nanosheets [22]. But the development of a low density, h-BN porous solid by the large scale, mutual linkage of functionalized h-BN sheets is

not yet realized, and such a porous solid, if it forms, will be useful in many applications including as solid thermal management material, as a spacer in 3D battery, selective organic absorption from water etc.

Here, a method for the functionalization of h-BN flakes is proposed and a covalent linkage between the flakes is attempted using an external cross-linking agent, glutaraldehyde (GAD). The developed porous monoliths were further studied for their structural and morphological properties along with their applicability in oil absorption.

Results and Discussion:

A method similar to the ‘Improved method’, for the development of graphene oxide from graphite, was adopted for the functionalization of h-BN [23] (*supporting information*). Commercial h-BN (1 μ m size, 98% pure, Sigma Aldrich) was used as the starting material. The h-BN foam was synthesized through the chemical cross-linking of functionalized individual h-BN flakes. The functionalized h-BN (i-hBN) was dispersed in deionized water (5mg/mL) and treated with resorcinol (11mM) and GAD (22mM). The resulting viscous fluid like material was sonicated (135 W, 28 °C) for 3 hours. This slurry was then subjected to lyophilization for 24 hours which resulted in to a white low density (bulk density \sim 40 mg/cm³) solid of h-BN as shown in figure 1A.

The XRD pattern of h-BN foam (*supporting information SI*) resembles that of bulk h-BN. The porosity of the h-BN foam is evident from the Field Emission Scanning Electron Microscope (FESEM) images shown in figure 1B and 1C. The SEM images indicate interconnected porous nature of the white solid with ‘macropores’ (pore size > 50 nm) structure.

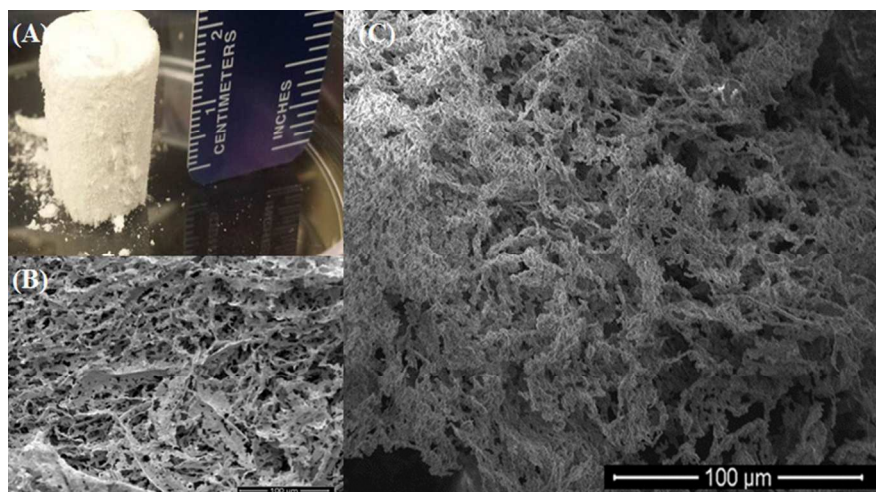


Figure 1. (A) Photograph of h-BN foam. The size of the foam is shown *via* the adjacent scale. (B) and (C) are the FESEM images of the same foam showing the microscopic structure of the h-BN foam.

Further, Transmission Electron Microscope (TEM) images of the h-BN foam taken after dispersing it in acetone using a mild sonication is shown in figure 2A. Presence of many layered disordered structure of h-BN flakes is evident from the image. This indicates that the ‘Improved method’ could not completely exfoliate h-BN unlike in the case of graphite oxide. Further, thermo-gravimetric (TG) analysis (Figure 2C) was carried out in air on h-BN and i-hBN. It is clear from the analysis that pristine h-BN is stable in air up to $\sim 750^{\circ}\text{C}$ but chemically modified h-BN (i-hBN) started disintegrates above 230°C , which is attributed to the removal of oxygen containing groups ($\sim 25\%$ removal by 750°C). TGA study on the h-BN foam is shown in figure 2C (down). Here, the functional moieties start disintegrating from low temperatures (below 100°C) onwards, which can be due to the surface adsorbed water molecules in the highly functionalized and porous h-BN foam, and it continues to do so up to a temperature of 450°C (40% removal). The presence of other oxygen containing groups (which is further evident from

FTIR spectra, figure 3) induced by the cross-linking process also make the decomposition in this temperature window.

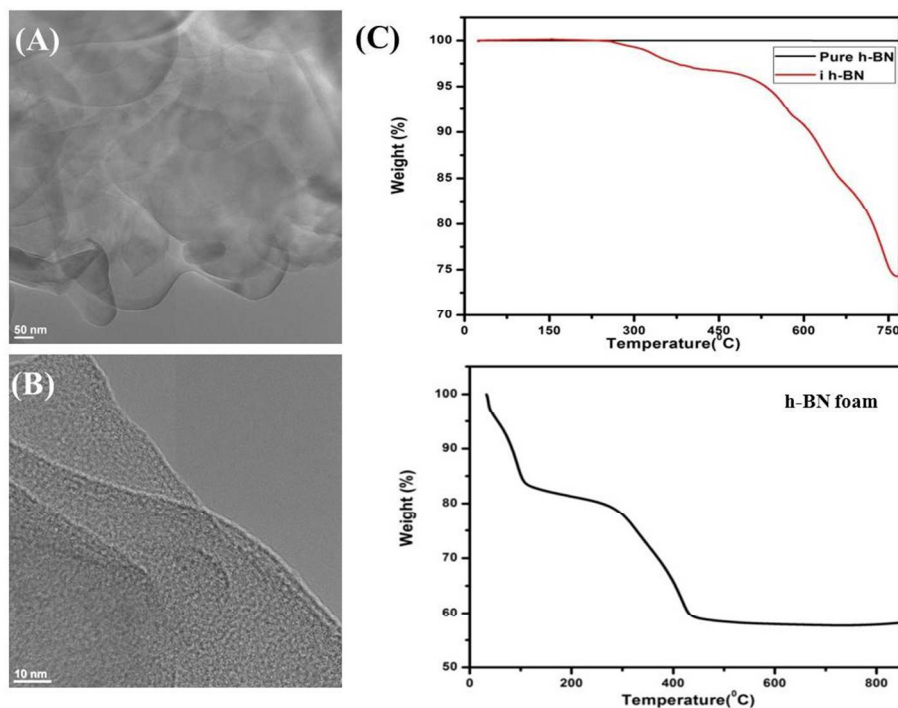


Figure 2. (A) TEM and (B) HRTEM image of h-BN foam. (C) TGA of pristine h-BN, i-hBN and h-BN foam

To further probe on the chemical functionalization, Fourier Transform Infrared Spectroscopy (FTIR) study was conducted, and the spectra of h-BN, i-hBN and h-BN foam are compared in figure 3. The presence of oxygen bearing functional groups is clear from the FTIR spectra of i-hBN and h-BN foam. Other than the characteristic peaks of B-N, the spectrum of h-BN foam contains peaks corresponding to B-N-O at 1165 cm^{-1} and 959 cm^{-1} . The peak at 1100 cm^{-1} corresponds to the B-O-H in plane bending. It was reported that in FTIR spectrum for h-BN, it is difficult to find the functionalities because of their prominent high intense B-N peaks at 817 cm^{-1} and 1370 cm^{-1} and that can be overlapped with other vibrations [24]. However in the

present case of h-BN foam, the functional peaks are clear and distinct. The presence of an additional functional group at $\sim 2900\text{ cm}^{-1}$ corresponding to $-\text{CH}$ stretching indicates the hemiacetal linkage in h-BN foam as previously reported in the case of GO foam [17]. A considerable red shift in the $-\text{OH}$ stretching frequency in h-BN foam compared to i-hBN (i h-BN) also indicates the covalent linkage via hemiacetal formation. This establishes the covalent linkages between individual h-BN flakes *via* hemiacetal linkage due to the hydroxyl groups in h-BN flakes and aldehyde groups in cross-linking agent GAD, resulting in a porous solid.

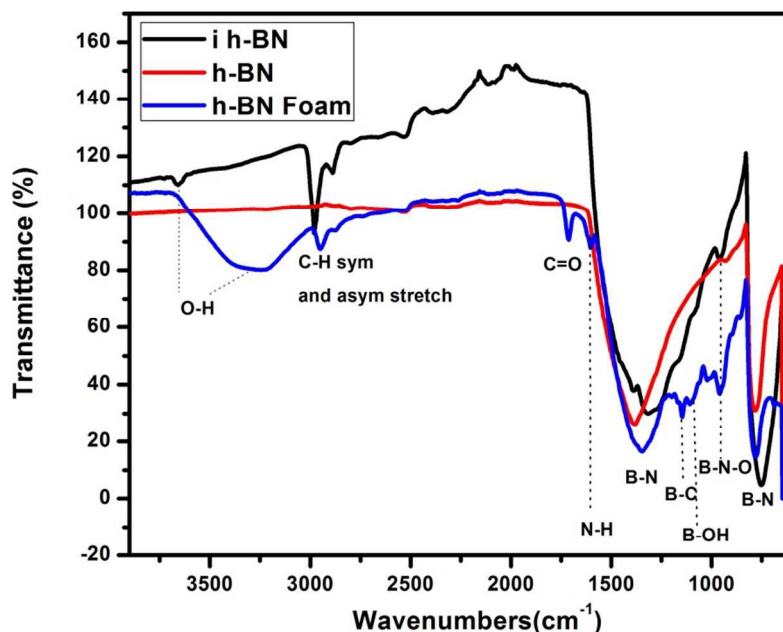


Figure 3. FTIR spectra of h-BN, i-hBN and h-BN foam, comparing the functionalities of h-BN foam with pure h-BN powder and functionalised h-BN.

In addition, a deconvoluted XPS slow scan spectra of B 1s, N 1s, O 1s and C 1s unravel (Figure 4) the chemical structure of h-BN foam. Using CASA XPS software, atomic ratios of B, C, N and O were estimated as 1.2:0.11:1:0.08 respectively in the case of i-hBN, and as 1.2:0.45:1:0.23 in h-BN foam. The small amount of carbon content is from the amorphous

carbon network formation by the Resorcinol-GAD cross-linking. Moreover, the shoulder peaks in B, C, N and O are associated with B-O, B-C, N-O, B-N and C-O bonding is in agreement with FTIR analysis. The survey scan XPS spectra of pure h-BN and h-BN foam are shown in figure S2 (*Supporting information*). The absence of oxygen in h-BN (pristine) is evident from the survey scan, while h-BN foam XPS spectrum showed considerable amount of oxygen, indicating the oxygen functionalization on h-BN after treatment.

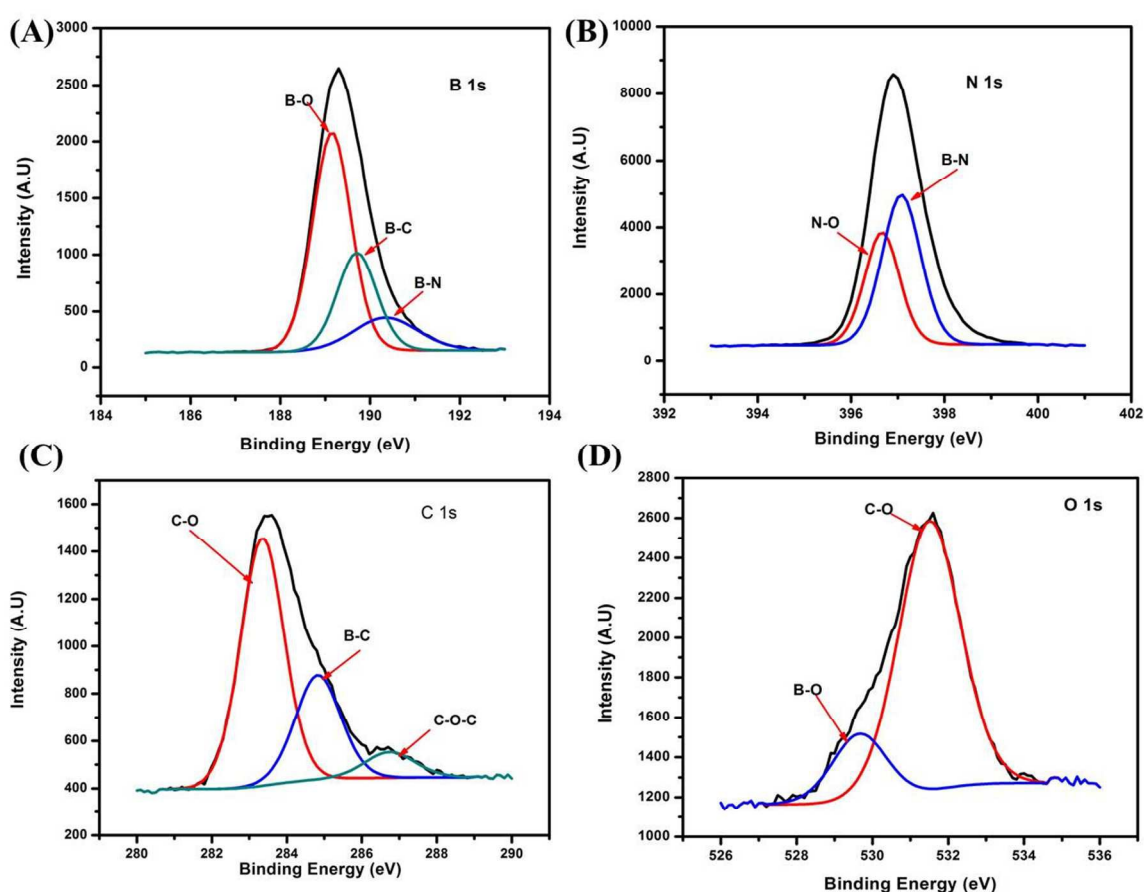


Figure 4. Deconvoluted XPS Spectra: (A) B 1s (B) N 1s (C) C 1s and (D) O 1s of 3D h-BN foam.

To further investigate the hydrophobicity of h-BN, contact angle measurement was carried out and is exhibited in figure S3 (*supporting information*). Pristine h-BN (commercial)

shows hydrophobicity with a contact angle of 130° , as reported in literature [25]. But in the case of h-BN foam, water is wetting the surface, indicates the increased amount of oxygen functionalities at the surface.

Nitrogen adsorption-desorption isotherms (Figure.5) of h-BN foam were measured using a Quantachrome NOVA 3000 instrument at 77 K. The h-BN foam was outgassed at 200 °C for 2 hours in dynamic vacuum before each measurement.

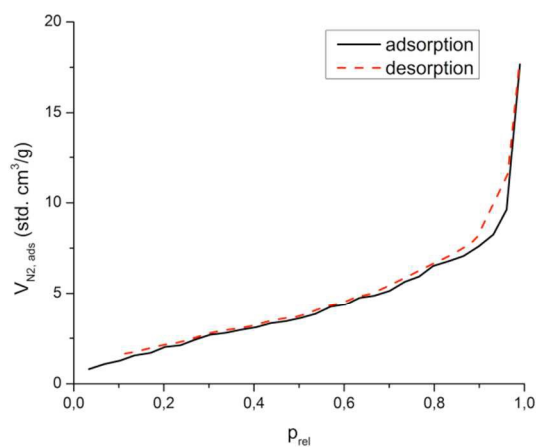


Figure 5. The adsorption-desorption isotherm pairs of h-BN foam.

h-BN foam exhibited an IUPAC Type II isotherm which is characteristic of either non-porous or macroporous adsorbents. The isotherms are linear at very low relative pressure upto the inflection point, $P_{rel} > 0.9$ where N_2 condensation finally occurs. This is a macroporous structure built up of flat lamellae separated by several hundreds of nanometers. The layers forming these macropore walls are non-porous themselves. A macro-world analogue of this structure would be a house of cards.

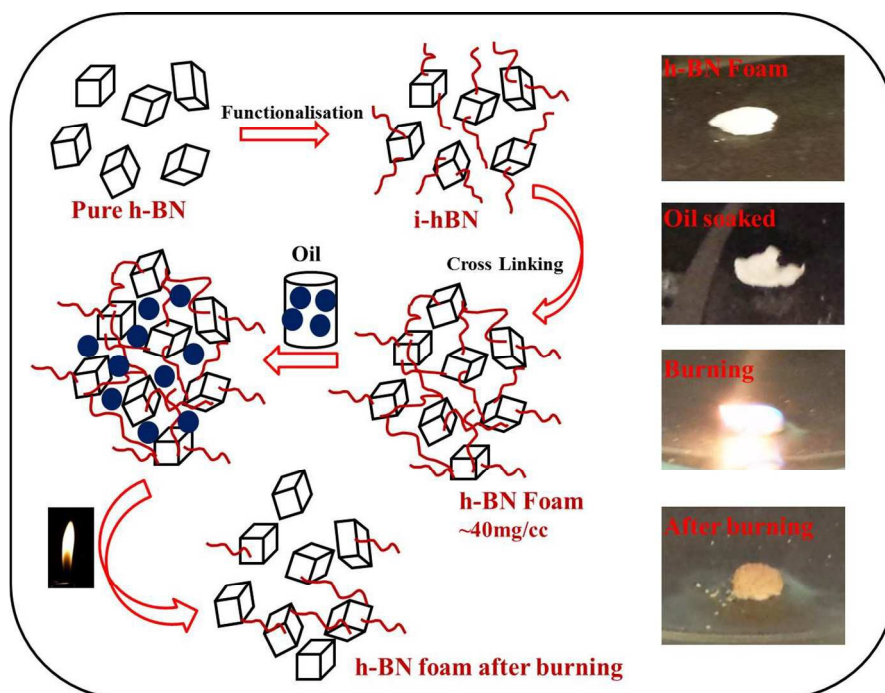


Figure 6. Schematic of the h-BN foam development and its oil adsorption and burning. Real time images of the oil (used engine oil) soaking and later burning of the foam are shown on the right.

One of the advantages of h-BN is its high thermal stability in air. These macro-porous monoliths were demonstrated for oil absorption (Figure.6). The complete soaking of the foam in oil resulted in the holding of 2g/g (2g used engine oil in 1g foam, this value is similar to the commercial polymer beds used in oil recovery field [26]) oil. After careful removal of the un-adsorbed surface oil, burning of the adsorbed oil in air is conducted as shown in figure 6. The FTIR spectrum of the residual h-BN foam after the complete burning of the oil is shown in figure 7. It is observed that even after the burning of soaked oil, h-BN foam still has functional groups such as –OH and –CH stretching bonds along with the characteristic BN bonds as discussed in the previous section indicating the structural integrity of the developed h-BN foam.

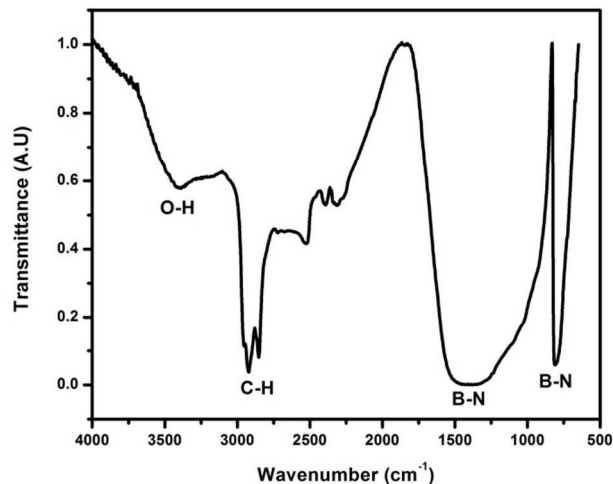


Figure 7. FTIR spectrum of h-BN foam after the burning of absorbed oil.

In conclusion, a method for the development of functionalized h-BN was pursued and oxygenated h-BN flakes were developed in bulk. These h-BN flakes were covalently bonded together using GAD-resorcinol cross-linking chemistry to obtain a low density macro-porous h-BN monolith solid (foam). The structural integrity, chemical functionalization and chemical structure of h-BN foams were studied using XRD, FESEM, FTIR and XPS analyses. This functionalization approach and template free bulk method for the synthesis of h-BN porous solids open new avenues for h-BN in applications such as corrosion resistive stable coatings, filter membranes, thermal foam, selective oil adsorption beds and spacers in 3-dimensional batteries. One such application is demonstrated here showing the capability of holding organic contaminants in porous h-BN and their further burning without oxidizing or disrupting the h-BN skeleton.

Acknowledgements:

P.M.S and T.N.N acknowledge the financial support from TIFR-Centre for Interdisciplinary Sciences. TNN acknowledges DST for financial support in the form of DST-FAST Track

scheme (SB/FTP/PS-084/2013). P.M.S, S.V, R.S, R.V and P.M.A acknowledge the U.S. Department of Defense: U.S. Air Force Office of Scientific Research for the Project MURI: “Synthesis and Characterization of 3-D Carbon Nanotube Solid Networks” Award No. FA9550-12-1-0035. A.K and Z.K acknowledge the financial support of the OTKA NN 110676 and K 112531 projects.

Reference:

1. A. Nag, K. Raindogia, K. P. S. S. Hembram, R. Datta, U. V. Wangmare, C. N. R. Rao, *ACS Nano*. 2010, **4**, 1539–1544.
2. K. S. Novoselov, D. Jiang, F. Schedin, T. J. Booth, V. V. Khotkevich, S. V. Morozov, A. K. Geim, *Proc. Natl. Acad. Sci. U.S.A.*, 2005, **102**, 10451–10453.
3. B. Radisavljevic, A. Radenovic, J. Brivio, V. Giacometti, A. Kis, *Nat. Nanotechnol.*, 2011, **6**, 147–150.
4. C. R. Dean, A. F. Young, I. Meric, C. Lee, L. Wang, S. Sorgenfrei, K. Watanabe, T. Taniguchi, P. Kim, K. L. Shepard, J. Hone, *Nat. Nanotechnol.* 2010, **5**, 722–726.
5. R. Arenal, X. Blase, A. Loiseau, *Adv. Phys.* 2010, **59**, 101–179.
6. Han, W.-Q. *Anisotropic Hexagonal Boron-Nitride Nanomaterials: Synthesis and Applications. Nanotechnologies for the Life Sciences*; Wiley: New York, published online Oct. 15, 2010.
7. Y. Hernandez, V. Nicolosi, M. Lotya, F. M. Blighe, Z. Sun, S. De, I. T. McGovern, *et.al.* *Nat. Nanotechnol.* 2008, **3**, 563–568.
8. J. N. Coleman *et.al*; *Science*, 2011, **331**, 568–571.
9. Umar Khan, Arlene O'Neill, Mustafa Lotya, Sukanta De and J. N. Coleman, *Small*, 2010 **6**, 7, 864–871.

10. D. Golberg, Y. Bando, Y. Huang, T. Terao, M. Mitome, C. Tang, C. Zhi, *ACS Nano*, 2010, **4**, 2979–2993.
11. A. Pakdel, C. Zhi, Y. Bando, T. Nakayama, D. Golberg, *ACS Nano*, 2011, **5**, 6507–6515.
12. J. Yu, L. Qin, Y. Hao, S. Kuang, X. Bai, Y. M. Chong, W. Zhang, E. Wang, *ACS Nano*, 2010, **4**, 414–422.
13. J. C. S. Wu, Z. A. Lin, J. W. Pan, M. H. Rei, *Appl. Catal. A*, 2001, **219**, 117–124.
14. Y. Xue, Q. Liu, G. He, K. Xu, L. Jiang, X. Hu, and J. Hu. *Nanoscale. Res. Lett*, 2013, **8**, 49.
15. Y. Lin, T. V. Williams, T. B. Xu, W. Cao, H. E. Elsayed-Ali, J. W. Connell, *J. Phys. Chem. C*, 2011, **115**, 2679–2685.
16. S. Vinod, C. S. Tiwary, P. A. S. Autreto, J. Taha-Tijerina, S. Ozden, A. C. Chipara, R. Vajtai, D. S. Galvao, T. N. Narayanan, P. M. Ajayan. *Nat. Communications* 2014, **5**, 4541.
17. P. M. Sudeep, T. N. Narayanan, A. Ganesan, M. M. Shaijumon, H. Yang, S. Ozden, et al. *ACS Nano*, 2013, **7**, 8, 7034–7040.
18. M. R. Philip, T. N. Narayanan, S. Bhushan Arya, D. K. Pattanayak, *J. Mater. Chem A*, 2014, **2**, 19488-19494.
19. W. Wang, Y. Bando, C. Zhi, W. Fu, E. Wang, D. Golberg, *J. Am. Chem. Soc*, 2008, **130**, 8144–8145.
20. C. Zhi, Y. Bando, C. Tang, D. Golberg, *J. Am. Chem. Soc*, 2005, **127**, 17144–17145.
21. Y. Lin, T. V. Williams, J. W. Connell, *J. Phys. Chem. Lett*, 2010, **1**, 277–283.
22. T. Sainsbury, A. Satti, P. May, Z. Wang, I. McGovern, Y. K. Gun'ko, J. Coleman, *J. Am. Chem. Soc*, 2012, **134**, 18758–18771.

23. D. C. Marcano, D. V. Kosynkin, J. M. Berlin, A. Sinitskii, Z. Sun, A. Slesarev, et al.
ACS Nano, 2010, **4**, 4806–4814.
24. A. S. Nazarov, V. N. Demin, E. D. Grayfer, A. I. Bulavchenko, A. T. Arymbaeva, H. Shin, Jae-Young Choi, V. E. Fedorov. *Chem. Asian J*, 2012, **7**, 554 – 560.
25. E. Hussain, T. N. Narayanan, Jaime-Taha Tijerena, S. Vinod, R. Vajtai and P M Ajayan.
ACS Appl. Mater. Interf., 2013, **5**(10), 4129-4135.
26. P. Thanikaivelan, T. N. Narayanan, B. K. Pradhan, P. M. Ajayan. *Sci. Reports*. 2012, **2**.